Camera Self-Calibration from Ellipse Correspondences

Rong Hu and Qiang Ji[†]
Department of Computer Science
University of Nevada, Reno
Department of Electrical, Computer and Systems Engineering[†]
Rensselaer Polytechnic Institute
qji@ecse.rpi.edu

Abstract

In this paper, we introduce a new technique for camera self-calibration using ellipse correspondences. Based on an analysis of ellipse matches between the images obtained from the same viewpoint but with different and unknown view directions, our approach estimates the intrinsic camera parameters. We present both liner and non-linear solutions to recovering intrinsic camera parameters. The algorithm's performance is validated extensively using both synthetic and real image data. Compared with similar techniques but using points, we observe a comparable performance. The use of ellipses, however, greatly simplifies feature matching between images, improves matching accuracy, and avoids mismatch.

1 Introduction

Camera calibration is an essential step for many robotics applications. It allows to extract metric information from 2D images. The purpose of camera calibration is to estimate the camera internal parameters including focal length, principle points, and scale factors.

Calibration methods used nowadays can be generally categorized into two classes ([21]): the traditional *test-field calibration* and the new *self-calibration.* Test-field calibration approach determines the camera parameters using a set of control geometric entities in both 2D and 3D. The entities may include points [15, 22, 18, 6], lines[7], ellipses[10] or a combination of different types of geometric entities [10]. The challenge with the traditional camera calibration approach is that it requires that the calibration object in 3D space is known with very good precision. This may not be feasible for certain applications. For example, for space applications such as the Mars-Rover it might be inconvenient or even impossible to carry with it such a calibration apparatus [23]. This has led to the recent development in self camera calibration.

In contrast with the traditional camera calibration, self camera calibration does not need 3D information of the calibration object. Camera parameters are estimated using multiple images of the calibration object from different viewpoints and/or view orientations. The idea with camera self calibration is that if images are taken by the same camera with fixed internal parameters, correspondences between these images are sufficient to calibrate a camera.

Most self camera calibration methods require camera to undergo a special movement. This tends to significantly simplify the solution and yield a more stable and robust solution. Two most common approaches of self camera calibration are purely translational [4] and purely rotational approaches [3, 5, 9]. Methods based on purely rotational camera movement have been proved to be very feasible and received most attention. According to this approach, multiple images of a scene are obtained by making the camera undergo only rotational movement while remain fixed in the same viewpoint. Camera calibration is then performed using the images. The major advantages of this approach include its algorithmic simplicity and operational simplicity. It can be easily implemented in practice. Hartley[8], Agapito [1] and Mendonca [14] presented calibration methods for a camera undergoing purely rotational movement. In [8], a camera with fixed intrinsic parameters can be calibrated by using at least three images of a 3D object obtained from the same point in space. They presented both an non-iterative and an iterative algorithms without the knowledge of the camera orientations. Agapito and Mendonca [1, 14] extended Hartley algorithm to allow changing of internal parameters. To decrease the sensitivity of self-calibration, Mendelsohn [13] advocates a constrained self-calibration method by placing small, planar, easily identifiable targets of known shape in the environment. The shapes of the targets are used to constrain the solutions, making them more robust.

Most of the existing methods for self-calibration rely on information equivalent to a passive 3D projective scene reconstruction (passive stereo). They therefore inherent the problems that plagued the stereo approach. For example, these methods are based on the point matchings, there is the issue of finding matched points in images taken from different viewpoints. This task can become more difficult because of the changes of aspects and lighting caused by camera movement. Moreover, the point-based methods usually need many points to improve robustness and accuracy, this tends to further aggravate the point matching problem.

In view of these problems, we introduce a new method to perform camera self calibration using ellipses. Ellipses have attracted the attention of researchers in the computer vision community as a useful symbol for camera calibration and pose estimation [10, 12, 19]. The main reasons are as follows: First, many man-made structures contain elliptical features and many objects can be represented by an ellipse. It can be especially useful in industrial environments, where circular holes are abundant. Second, like points and straight lines , ellipse are preserved under perspective or projective transformations. Third, an ellipse representation in mathematics is a symmetric matrix and is easy to implement. Ellipses contain compact global information, they are expected to be more robust to noise than points. It tolerates partial occlusion. Fourth, there is a wealth of theoretical studies on ellipses and these theories can be used. Finally, ellipses allow very reliable and precise feature-based matching ([19]). Correspondences can be much more easily established between ellipses.

Although ellipses have been employed for *test-field calibration*, to the best of our knowledge, it has not been used for self-calibration. The downside of using ellipses is that they are planar. It is known the solution is very sensitive to noise whenever planar or near-planar scenes occur since fundamental matrices can not be estimated stably in the near-planar case. But planar self-calibration has some potential advantages. Planes are very common in man-made environments and are simple to process. Moreover, recent research has improved the performance of planar self-camera calibration [20, 2].

In this paper, we present a new pure rotational self-calibration method using ellipse. For the research described in this paper, we assume the camera has a fixed interior parameters and that the radial distortions can be ignored. We also assume the camera undergoes a purely yet unknown rotational movement to obtain different images. This paper is organized as follows: In section 2, we introduce some notations and lay the mathematical background for perspective projection of ellipses. The mathematical model for ellipse-based self-calibration is discussed in section 3. Section 4 shows experimental results to validate the proposed camera self calibration technique using ellipses with both synthetic and real image data. The paper ends in section 4 with a summary and conclusions.

2 Notations and Perspective Projection of Ellipses

As shown in Figure 1, let X-Y-Z represent the object coordinate frame. The origin of the object frame is located at the center of the 3D ellipse, and the X and Y axes are along the major and minor axes of the ellipse. The Z axis is perpendicular to the 3D ellipse plane. Let $\mathbf{X}_m = [X \quad Y \quad 0]^T$ be the coordinates of an ellipse point in 3D and $\mathbf{P} = [c\ r]^T$ be the pixel coordinates of the corresponding image point.

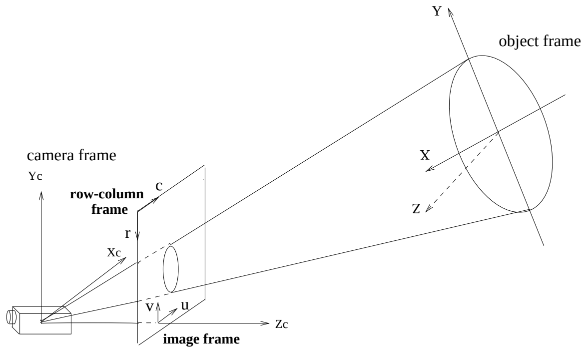

Figure 1. Camera perspective projection model

From the pinhole perspective projection model, in homogeneous coordinate system we have

$$\lambda \begin{pmatrix} c \\ r \\ 1 \end{pmatrix} = \mathbf{W}[\mathbf{R} \quad \mathbf{T}] \begin{pmatrix} X \\ Y \\ 0 \\ 1 \end{pmatrix} \tag{1}$$

where, $\mathbf{R}$ is a rotation matrix and $\mathbf{T}$ is a translation vector, and λ is an unknown scaler. They characterize the relative orientation and position of object frame to the camera coordinate frame (X_c-Y_c-Z_c). $\mathbf{W}$ is called the camera intrinsic matrix, denoted as

$$\mathbf{W} = \begin{pmatrix} s_x f & 0 & u_0 \\ 0 & s_y f & v_0 \\ 0 & 0 & 1 \end{pmatrix}$$

where s_x and s_y are scale factors (pixels/mm), f for focus length, u_0, v_0 are the coordinates of the principle point in pixels. Equation 1 may be rewritten as

$$\lambda \begin{pmatrix} c \\ r \\ 1 \end{pmatrix} = \mathbf{W}[\mathbf{r}_1 \ \mathbf{r}_2 \ \mathbf{T}] \begin{pmatrix} X \\ Y \\ 1 \end{pmatrix} \quad (2)$$

where $\mathbf{r_1}$ and $\mathbf{r_2}$ are the first two columns of matrix $\mathbf{R}$. Denote $\mathbf{G} = [\mathbf{r}_1 \ \ \mathbf{r}_2 \ \ \mathbf{T}]$, $\mathbf{G}$ is called the camera extrinsic matrix and equation 2 is rewritten

$$\lambda \begin{pmatrix} c \\ r \\ 1 \end{pmatrix} = \mathbf{WG} \begin{pmatrix} X \\ Y \\ 1 \end{pmatrix} \quad (3)$$

(3) is the projection equation that characterizes the relation between an image ellipse point and the corresponding 3D ellipse point.

Let $\mathbf{Q}$ be a 3×3 matrix representing the 3D ellipse in object frame, $\mathbf{A}$ be a 3×3 matrix for the image ellipse, the equations of the image ellipse and the 3D ellipse respectively are

$$\begin{pmatrix} c \\ r \\ 1 \end{pmatrix}^T \mathbf{A} \begin{pmatrix} c \\ r \\ 1 \end{pmatrix} = 0 \quad (4)$$

$$\begin{pmatrix} X \\ Y \\ 1 \end{pmatrix}^T \mathbf{Q} \begin{pmatrix} X \\ Y \\ 1 \end{pmatrix} = 0 \quad (5)$$

Substituting eq. (3) to eq. (4) and after simplification leads to

$$\begin{pmatrix} X \\ Y \\ 1 \end{pmatrix}^T \lambda \mathbf{G}^T \mathbf{W}^T \mathbf{AWG} \begin{pmatrix} X \\ Y \\ 1 \end{pmatrix} = 0 \quad (6)$$

From (5) and (6), we have

$$\mathbf{Q} = \lambda \mathbf{G}^T \mathbf{W}^T \mathbf{AWG} \quad (7)$$

Equation 7 is the basic projective equation that relates a 3D ellipse to its projection and to the exterior and interior camera parameters.

3 Camera Self-Calibration with Ellipses

In this section, we will present the mathematical theories for camera self-calibration using image ellipses obtained with camera undergoing pure but unknown rotational movement. We will present a linear method as well as a non-linear method. In each case, we assume the rotational motion that the camera undergoes from one to another view is unknown. This is because the relative orientation is difficult to estimate accurately. The use of inaccurate relative orientation may lead to significant errors. Our method is, however, general enough to be able to incorporate $\mathbf{R}$ in the computation if it can be obtained accurately.

3.1 Linear algorithm

Following the same notations as introduced in section 2, let $\mathbf{Q}$ be a 3×3 matrix representing a 3D ellipse and $\mathbf{A_1}$ and $\mathbf{A_2}$ be the two image ellipses of $\mathbf{Q}$. From equation 7, we have

$$\lambda \mathbf{G_1^T W^T A_1 W G_1} = \mathbf{G_2^T W^T A_2 W G_2} \quad (8)$$

where $\mathbf{G_1} = (\mathbf{r_{11}} \ \mathbf{r_{12}} \ \mathbf{T_1})$, $\mathbf{G_2} = (\mathbf{r_{21}} \ \mathbf{r_{22}} \ \mathbf{T_2})$, and $\mathbf{r_{11}} \ \mathbf{r_{12}}$ and $\mathbf{r_{21}} \ \mathbf{r_{22}}$ are respectively two left columns of $\mathbf{R_1}$ and $\mathbf{R_2}$, which specify relative orientation of two views relative to the object frame. Since the relationship between the two images is pure rotation, i.e: $\mathbf{R_2} = \mathbf{RR_1}$, $\mathbf{T_2} = \mathbf{RT_1}$. As a result, we have $\mathbf{G_2} = \mathbf{RG_1}$. Substituting it into equation 8 yields

$$\lambda \mathbf{G_1^T W^T A_1 W G_1} = \mathbf{G_1^T R^T W^T A_2 W R G_1} \quad (9)$$

Equation (9) leads to

$$\lambda \mathbf{W^T A_1 W} = \mathbf{R^T W^T A_2 W R} \quad (10)$$

Equation 10 can be rewritten as

$$\lambda \mathbf{A_1} = (\mathbf{WRW^{-1}})^\mathbf{T} \mathbf{A_2} (\mathbf{WRW^{-1}}) \quad (11)$$

Equation 11 is the fundamental equation for ellipses (similar to the fundamental equations for points in stereo).

Using the fact that $Det(\mathbf{WRW^{-1}})$=1, the scaler λ in equation 11 can be obtained from $\lambda = (\frac{Det(\mathbf{A_2})}{Det(\mathbf{A_1})})^{1/3}$. Let $\mathbf{K} = \mathbf{WRW^{-1}}$ and assuming λ is solved, equation 11 can be rewritten as

$$\mathbf{A_1} = \mathbf{K^T A_2 K} \quad (12)$$

It is apparent from equation 12 that solution to $\mathbf{K}$ is non-linear. To obtain a linear solution, we need another 3D ellipse. Suppose there are two 3D ellipses $\mathbf{Q_A}$ and $\mathbf{Q_B}$, $\mathbf{A_1} \ \mathbf{A_2}$ and $\mathbf{B_1} \ \mathbf{B_2}$ are the corresponding image ellipses obtained from two different views. Then following equation 12, we have

$$\begin{aligned} \mathbf{K^{-T}} &= \mathbf{A_2 K A_1^{-1}} \\ \mathbf{K^{-T}} &= \mathbf{B_2 K B_1^{-1}} \end{aligned} \quad (13)$$

Note the two ellipses share the same $\mathbf{K}$ since the camera undergoes the same rotational movement and therefore they share the same $\mathbf{R}$.
From Equation (13), we have

$$\mathbf{A_2 K A_1^{-1}} = \mathbf{B_2 K B_1^{-1}} \quad (14)$$

In Eq. (14), only $\mathbf{K}$ is unknown, we can see that $\mathbf{K}$ can be linearly solved. However, since $\mathbf{K}$ appears on both sides of equation 14, $\mathbf{K}$ can only be solved for up a scale factor as explained in [17]. In order to find an unique solution to $\mathbf{K}$, we need to obtain two such equations as equation 14. It means that we need at least three ellipses in the same image. Assuming there is another ellipse $\mathbf{Q_C}$ in the object frame, $\mathbf{C_1}$ $\mathbf{C_2}$ are the corresponding image ellipses. Between ellipses $\mathbf{Q_A}$ and $\mathbf{Q_C}$, there exists

$$\mathbf{A_2KA_1^{-1}} = \mathbf{C_2KC_1^{-1}} \tag{15}$$

Equations 14 and 15 offer a total of 18 independent linear equations involving 9 unknowns in $\mathbf{K}$. The system of linear equations is therefore over-determined. $\mathbf{K}$ can hence be solved linearly. Once $\mathbf{K}$ is solved, we can solve for $\mathbf{W}$.

To solve for $\mathbf{W}$, we utilize the orthnormality constraint of $\mathbf{R}$, i.e., $\mathbf{R} = \mathbf{R^{-T}}$. From $\mathbf{K} = \mathbf{WRW^{-1}}$, we have $\mathbf{R} = \mathbf{W^{-1}KW}$ and $\mathbf{R^{-T}} = \mathbf{W^TK^{-T}W^{-T}}$. Thus,

$$(\mathbf{WW^T})\mathbf{K^{-T}} = \mathbf{K}(\mathbf{WW^T}) \tag{16}$$

Let $\mathbf{S} = \mathbf{WW^T}$, equation 16 can be changed to

$$\mathbf{SK^{-T}} = \mathbf{KS} \tag{17}$$

where

$$\begin{aligned} \mathbf{S} &= \begin{pmatrix} s_x f & 0 & u_0 \\ 0 & s_y f & v_0 \\ 0 & 0 & 1 \end{pmatrix} \begin{pmatrix} s_x f & 0 & 0 \\ 0 & s_y f & 0 \\ u_0 & v_0 & 1 \end{pmatrix} \\ &= \begin{pmatrix} s_x^2 f^2 + u_0^2 & u_0 v_0 & u_0 \\ u_0 v_0 & s_y^2 f^2 + v_0^2 & v_0 \\ u_0 & v_0 & 1 \end{pmatrix} \end{aligned} \tag{18}$$

Equation 16 is so-called Kruppa equation [6]. To uniquely determine the solution to $\mathbf{S}$, we need at least two equations like equation 16, which can be obtained by rotating a camera twice or more. The new equations resulted from additional camera rotation, along with equation 16, can then be combined to robustly and linearly solve for elements of $\mathbf{S}$, which then leads to solution to $\mathbf{W}$. Once we get $\mathbf{S}$, the intrinsic parameters of the camera can be solved from it. By experiments, we found that above linear algorithm is very sensitive to noise. In order to improve the robustness of this algorithm, we proposed the following non-liner algorithm.

3.2 Non-linear Algorithm

Given $\mathbf{K}$, equation 16 leads to nine non-linear equations for the four intrinsic cameras $s_x f$, $s_y f$, u_0, and v_0. The system is over-determined though the solution is non-linear. In this iterative algorithm, we use *downhill simplex method* [16]. The criterion function to

Table 1. Self-camera calibration results with the linear techniques. The ideal camera parameters are $s_x f = 420$, $s_y f = 410$, $u_0 = 160$, $v_0 = 120$. Each row represents results from a particular camera rotation sequence.

$s_x f$	$s_y f$	u_0	v_0	RMS
419.6203	479.4885	159.6781	119.6565	0.40
419.8934	479.7814	159.8191	119.8253	0.17
419.2015	478.7215	159.2577	119.3060	0.91
406.1907	462.8008	147.9237	110.9267	13.37

minimize is defined as follows. Let $\mathbf{V} = \mathbf{SK^{-T}} - \mathbf{KS}$ and V_{ij} be the $(i,\ j)$ entry of the matrix $\mathbf{V}$. The criterion function F we use to minimize to solve for intrinsic camera parameters is

$$\begin{aligned} F &= |V_{00}| + |V_{01}| + |V_{02}| + |V_{10}| + |V_{11}| + \\ & \quad |V_{12}| + |V_{20}| + |V_{21}| + |V_{22}| \end{aligned} \tag{19}$$

As a result, using down hill simplex method with the criterion function in Eq. 19, we can iteratively solve for the fs_x, fs_y, u_0, and v_0. Please note that for the nonlinear solution we only need rotate the camera once. The initial estimate of the non-linear procedure may be provided by the linear procedure or using the camera parameters as provided by the camera manufacturer.

4 Experiments

In order to study the performance of the proposed methods, we conducted experiments using both synthetic and real image data. To generate synthetic data, three 3D coplanar ellipses were generated first, followed by projecting the 3D ellipses onto image planes to produce their images. Different images under different camera orientations were produced to study impact image noise and the number of camera rotations on the quality of the estimated camera parameters. For the synthetic image data, the ideal ground truth camera parameters are $sf_x = 420$, $sf_y = 410$, $u_0 = 160$, and $v_0 = 120$. All units for subsequent figures and tables are mm.

Table 1 shows the results from the linear algorithm with different rotation sequences. The result is satisfactory except the last row in Table 1, where large errors result from small rotational angles between camera views.

To study the performance of the linear method under different noise levels, we add additive Gaussian noise to the coordinates of image pixels that form the 2D image ellipses. The results from the data with noises are shown in Table 2. The motion of the camera involves rotations around X, Y, Z axes respectively. We can see the algorithm is very sensitive to noise. This is because that there is no any object information to control the results. To improve the performance of the linear method, we increase the number ellipses and the number of images, the improvement, however, is not satisfactory.

4.0.1 Non-linear algorithm

We perform the same experiments to evaluate the performance of the non-linear algorithm. A general camera rotation results from rotating the camera sequentially around the three fixed major axes. To study the effect of camera rotation on the performance of the algorithm, we performed two types of rotation: rotating the camera sequentially around the three axes X, Y, and Z and rotating only around X and Y as indicated in the Figs. 2 and 3. The results from the non-linear algorithm based on 3 ellipses and one camera rotation are shown in Figure 2 and Figure 3. We can see the robustness of the algorithm to noise is significantly improved, as the noise is increased to 0.8, the results are still acceptable. This represents a significant improve over the linear method. The accuracy and robustness of the non-linear algorithm will be improved further if more ellipses and more rotations are applied.

4.1 Real data

The camera to be calibrated is a CDD camera. The image resolution is 640×480. We only used real data to test our non-linear method. We drew an ellipse on a 26 cm $\times$ 28 cm model plane, and duplicated it to obtain three ellipses. Then we pasted the three ellipses to a wall. Two images of the three ellipses were taken under different orientation of the camera by only rotating the camera once, as shown in Figure 4. Ellipses are detected using our ellipse detection method [11]. The distance between the camera and object ellipses is about 2.0 m. The calibration results are shown in the second row of Table 3. Since the ground truth of the camera intrinsic parameters is not known, we employed a classical method proposed in [22] to calibrate the same camera. The estimated camera parameters using the classical approach are shown in the first row of the Table 3 for comparison. We can see the two results are close. The ellipse-based algorithm without any knowledge of the orientation of the camera is verified by the reasonable result with real data.

5 Conclusions

In this paper, we introduce both a linear and nonlinear procedures for self camera calibration using ellipse correspondences. The performance of our algorithms is studied using both synthetic and real image data. The experiments reveal that it is possible to perform self-camera calibration using ellipses. The experiments show that while the linear solution is easy to solve and fast, it requires an additional camera rotations (twice) and its solution is sensitive to image noise unless additional images are used. The non-linear solution is more stable and robust. It is clear that the accuracy of the propsoed non-linear ellipse-based method is comparable to that of point-based methods. But the proposed ellipse-based method overcomes the point matching problem that plagued the point-based methods and is less sensitive to image noises. One problem with our approach is the lack of elliptical or circular features for certain scene. Ellipses are not so abundant as lines or points.

References

[1] L. Agapito, R.I.Hartley, and Eric Hayman. Linear calibration of a rotating and zooming camera. *IEEE Computer Society Conference on Computer Vision and Pattern Recognition*, 1(15-21), 1999.

[2] M. Armstrong, A. Zisserman, and R. Hartley. Self-calibration from image triplets. *the 4th European Conference on Computer Vision*, 1, 1996.

[3] A. Basu. Active calibration: Alternative strategy and analysis. *Proc. IEEE Conf. On Computer Vision and Pattern Recognition*, pages 495–500, 1993.

[4] L. Dron. Dynamic camera self-calibration from controlled motion sequences. *In Proc. IEEE Conf. On Computer Vision and Pattern Recognition*, 501-6, 1993.

[5] F. Du and M. Brady. Self-calibration of the intrinsic parameters of camers for active visio n systems. *Computer Vision and Pattern Recognition*, pages 477–482, 1993.

[6] O. D. Faugeras, O. T. Luong, and S. J. Maybank. Camera self-calibration: Theory and experiments. *ECCV'92, Lecture notes in Computer Science*, 588:321–334, 1992.

[7] R. Hartley. Camera calibration using line correspondences. *DARPA*, pages 361–366, 1993.

[8] R. Hartley. Self-calibration of stationary cameras. *International Journal of Computer Vision*, 22(1):5–23, 1996.

[9] R. Hartley. Self-calibration of stationary cameras. *International Journal of Computer Vision*, 22(1):5–23, 1997.

[10] Q. Ji, M. S. Costa, R. M. Haralick, and L. G. Shapiro. An integrated linear technique for pose estimation from different geometric features. *International Journal of Pattern Recognition and Artificial Intelligence*, 13(5):200–215, 1999.

[11] Qiang Ji and Robert M. Haralick. A statistically efficient method for ellipse detection. *in 1999 IEEE International Conference on Image Processing, Kobe, Japan, October*, 1999.

[12] S. D. Ma. Conics-based stereo, motion estimation, and pose determination. *International Journal of Computer Vision*, 10(1):7–25, 1993.

[13] J. Mendelsohn and K. Daniilidis. Constrained self-calibration. *IEEE Computer Society Conference on Computer Vision and Pattern Recognition*, 2:581–587, 1999.

Table 2. Noise influence on the calibration results under different noise levels

noise levels	$s_x f$	$s_y f$	u_0	v_0	RMS
0	419.6581	479.5017	159.6800	119.6686	0.38
0.01	398.9377	452.6379	141.3208	105.5467	20.92
0.02	354.9710	403.0581	108.8793	82.6817	59.49
0.03	314.0975	354.4728	83.2944	63.3038	94.96
0.04	228.6159	249.4738	42.7778	30.6545	166.95
0.05	197.1667	216.4344	31.9835	23.4944	190.28

Table 3. Real data experiment results

methods	$s_x f$	$s_y f$	u_0	v_0
classical	418.25367	413.938806	162.116273	118.024387
ellipse_based	439.999725	430.000031	189.999924	125.000076

[14] P. R. S. Mendonca and R. Cipolla. A simple technique for self-calibration. *IEEE Computer Society Conference on Computer Vision and Pattern Recognition*, 1:500–505, 1999.

[15] O.Faugeras. Three-dimensional computer vision: a geometric viewpoint. *MIT Press*, 1993.

[16] W. H. Press. Numerical recipes in c : the art of scientific. *Cambridge [England] ; New York : Cambridge University Press, 1997*, 1997.

[17] Y. C. Shiu and S. Ahmad. Calibration fo wrist-mounted robotic sensors by solving homogeneous transform equations of the form $ax = xb$. *IEEE Transactions on Robotics and Automation*, 5(1):16–28, 1989.

[18] P. F. Sturm and S. J. Maybank. On plane-based camera calibration: A general algorithm, singularities, applications. *IEEE Computer Society Conference on Computer Vision and Pattern Recognition*, 1:432–437, 1999.

[19] J. P. Tarel and A. Gagalowicz. Calibration de caméra à base d'ellipses. *Traitement du Signal*, 12(2):177–187, 1995.

[20] B. Triggs. Autocalibration from planar scenes. *the 5th European Conference on Computer Vision*, pages 89–105, 1998.

[21] G. Q. Wei, K. Arbter, and G. Hirzinger. Active self-calibration of robotic eyes and hand-eye relationships with model identification. *IEEE Transactions on Robotics and Automation*, 14(1):158–166, 1998.

[22] Z. Zhang. A flexible new technique for camera calibration. *Technical Report MSR-TR-98-71 http://research.microsoft.com/ zhang*, 1998.

[23] Z. Y. Zhang. Self-maintaining camera calibration in time. *http://www-sop.inria.fr/robotvis/personnel/vubs/calib/calib.html*, 1996.

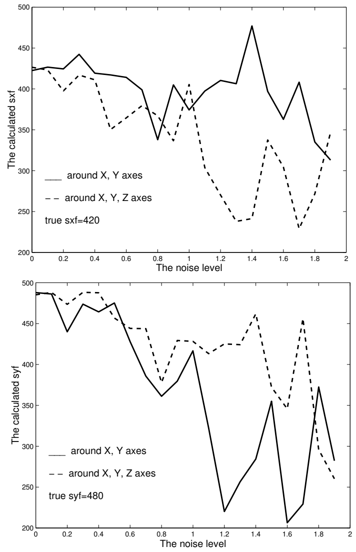

Figure 2. The estimated $s_x f$ and $s_y f$ using the non-linear algorithm as function of the noise levels. The results are obtained with 3 ellipses and one camera rotation

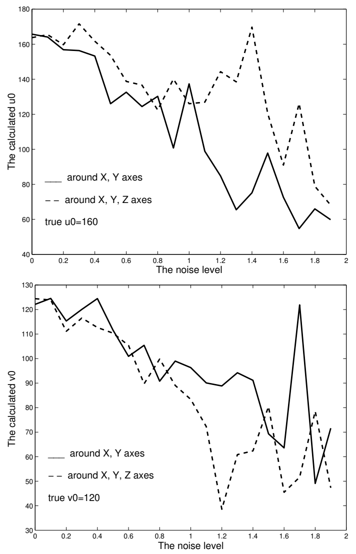

Figure 3. The estimated u_0 and v_0 from the non-linear algorithm as a function of noise levels. The results are obtained from 3 ellipses and one camera rotation.

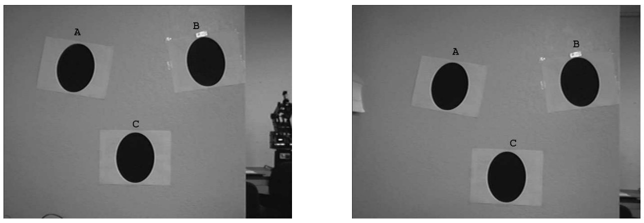

Figure 4. The real images obtained from two different view directions.